ANTIOXIDANTS & REDOX SIGNALING
Volume 11, Number 7, 2009

DOI: 10.1089/ars.2008.2393

Forum Original Research Communication

Role of NF-κB in Flow-Induced Vascular Remodeling

Yves Castier,[1,2] Bhama Ramkhelawon,[1] Stéphanie Riou,[1] Alain Tedgui,[1] and Stephanie Lehoux[1,3]

Abstract

Vascular remodeling associated with increased blood flow involves reactive oxygen species (ROS)-dependent activation of matrix metalloproteinases (MMPs). To investigate the potential role of NF-κB in this process, human umbilical vein endothelial cells were subjected to different flow conditions during a 24-h period. Normal (15 dynes/cm^2) and high (30 dynes/cm^2) shear stress induced IκBα degradation and NF-κB p65 phosphorylation, and activated MMP-2 and MMP-9. These effects were blunted in cells incubated with the NF-κB inhibitor pyrrolidine dithio-carbamate (PDTC). In mice, creation of a carotid artery–jugular vein arteriovenous fistula (AVF) increased carotid blood flow sixfold, triggering the increase in carotid diameter from 459 ± 8 μm (before AVF) to 531 ± 13 and 669 ± 21 μm (7 and 21 days after AVF). ROS production and NF-κB activity were enhanced in fistulated carotids, but only the latter was blocked by PDTC, although PDTC blocked ROS production *in vitro*. In PDTC-treated mice, changes in carotid caliber and shear stress matched controls at 7 days, but carotids enlarged only marginally thereafter, reaching only 578 ± 8 μm at 21 days ($p < 0.01$ *vs.* untreated). Similarly, both MMP-9 expression and activity were abrogated by PDTC at 3 weeks. Hence, induction of NF-κB by shear stress contributes to MMP induction and allows long-term flow-induced vascular enlargement. *Antioxid. Redox Signal.* 11, 1641–1649.

Introduction

Long-term changes in blood flow are associated with vascular remodeling, involving the reorganization of cellular and extracellular components, which tends to normalize shear stress. In conditions in which blood flow is substantially enhanced, as typified by models of arteriovenous fistula (AVF), the ensuing increase in diameter occurs through extensive tearing and fragmentation of the internal elastic lamina (17, 45), which augments arterial distensibility. We (6, 44) and others (1, 24) previously implicated matrix metalloproteinases (MMPs) in this process. MMPs, which are secreted as inactive zymogens (pro-MMPs), are rapidly cleaved and activated in *in vivo* models of prolonged increased blood flow and remain active until shear stress is normalized. Enhanced production of nitric oxide (NO) and reactive oxygen species (ROS) in high-flow conditions (18, 20, 44, 45), *via* endothelial NO synthase (eNOS) and NADPH oxidase (6), generates peroxynitrite, which is important for MMP cleavage (38) and essential to high flow–induced vascular remodeling (6).

The prolonged contribution of MMPs to the remodeling process likely implicates not only their activation but also their synthesis. In this regard, whereas some MMPs are constitutively produced in vascular cells, such as MMP-2, others, like MMP-9, are inducible. Both gelatinases are implicated in the early phase of flow loading in vessels (44), but at time points ranging from 1 week after creation of an AVF and beyond, MMP-9 appears to play the predominant role (6, 44), suggesting prolonged pro–MMP-9 production. As it happens, different pathways have been implicated in vascular mechanosensitive regulation of MMPs. In cultured endothelial cells, oscillatory flow was shown to increase MMP-9 *via* c-*myc* (2), whereas laminar shear-stress conditions repressed MT1-MMP, after activation of Sp1 (49). MT1-MMP was stimulated by cyclic strain, however (25). Other studies highlighted the role of NF-κB in regulating MMP-9 expression in vessels exposed to strain (8) or endothelial cells stimulated with varying degrees of oscillatory or laminar shear stress (16, 42). Because vascular remodeling in response to long-term high flow in the vessel involves both shear sensing at the endothelium and stretch signaling in the underlying smooth muscle cells (as the

[1]Parts Cardiovascular Research Center, Inserm U970, HEGP; and [2]Service de Chirurgie Vasculaire, Hôpital Bichat, Paris, France.
[3]Lady Davis Institute for Medical Research, McGill University, Montreal, Quebec, Canada.

vessel expands), we hypothesized that NF-κB might be a major mediator of the remodeling response observed in flow-loaded arteries.

Materials and Methods

Cell culture

Human umbilical vein endothelial cells (ECs) obtained from Promocell (Heidelberg, Germany) were used between passages 2 and 4. Cells were grown in culture medium supplemented with fetal calf serum (5%) and growth factors, according to the supplier's instructions. ECs were seeded onto 0.2% gelatin-coated microscope slides before shear-stress experiments and exposed to different flow regimens (0, 15, and 30 dynes/cm^2) for 24 h by using a parallel-plate chamber placed in an incubator (37°C, 95% O_2). Some cells were treated with pyrrolidine dithiocarbamate (PDTC, 10^{-4} to 10^{-7} *M*; Sigma, St. Louis, MO) or SN50 (AAVALLPAVLLALLAP-VQRKRQKLMP, 50 μg/ml; Upstate Biotechnology, Billerica, MA) added to the culture medium at the onset of the flow experiments.

Western blot

Cells were lysed in ice-cold buffer containing 20 m*M* Tris-HCl (pH 7.5), 5 m*M* EGTA, 150 m*M* NaCl, 20 m*M* glycerophosphate, 10 m*M* NaF, 1 m*M* sodium orthovanadate, 1% Triton X-100, 0.1% Tween 20, and protease inhibitors (Boehringer Mannheim, Mannheim, Germany). Detergent-soluble fractions were retained, and protein concentrations in samples were equalized by using a Bradford protein assay (Bio-Rad, Hercules, CA). Blots were incubated with anti-IκBα, anti-GAPDH (Santa Cruz, Santa Cruz, CA), or anti–phospho-p65 NF-κB (Ser536; Cell Signaling Technology, Ipswich, MA) antibodies. An enhanced chemiluminescence system was used as the detection method (ECL+, Amersham, Piscataway, NJ).

MMP activity, ROS production, and p65 phosphorylation in HUVECs

Gelatin zymography was performed as described previously (28) by using 10 μl of cell lysate per microgram of cells. Gelatinolytic activity was visualized as clear bands of lysis against a dark background. For *in situ* zymography of cells, ECs were fixed for 20 min in PBS containing 2% paraformaldehyde and then rinsed with PBS. Cells were then incubated at 37°C for 5 h with a fluorogenic gelatin substrate (DQ gelatin; Molecular Probes, Carlsbad, CA) dissolved to 25 μg/ml in zymography buffer (50 m*M* Tris-HCl, pH 7.4; 15 m*M* $CaCl_2$). Cells were then incubated with anti–phospho-p65 NF-κB for 1 h, followed by a secondary antibody (Molecular Probes). Cover slips were mounted with medium containing DAPI (Vector Laboratories, Burlingame, CA). Proteolytic MMP activity was detected as green fluorescence; phospho-p65 as red fluorescence, and nuclei as blue fluorescence. Dihydroethidine (2×10^{-6} *M*; Sigma) was topically applied to cells, and its transformation to oxy-ethidium in the presence of ROS was revealed as red fluorescence (585 nm).

Animal experiments

Experiments were performed in accordance with the European Community Standards on the Care and Use of Laboratory Animals and were approved by the local ethics committee. Adult male mice weighing 25–35 g were operated on aseptically under general anesthesia, by using a microscope, as described earlier (6). In brief, animals were anesthetized by using ketamine (0.2 mg/g IP) and xylazine (0.02 mg/g IP), and an end-to-side anastomosis was performed between the right jugular vein and common carotid artery (RCCA) with six interrupted 11-0 nylon sutures (Ethicon, Somerville, NJ). Fifteen control and 15 treated (50 mg/kg/day PDTC) mice were killed 0, 7, and 21 days after surgery (five mice per group). Later times were not investigated because mice develop stenosis at the site of anastomosis, and vessel patency is reduced in many animals as of 28 days (6). Furthermore, no data were collected from animals with compromised flow due to thrombotic obstruction or stenosis. Arterial pressure and heart rate were measured with tail-cuff plethysmography (Visitech, Apex, NC) before and at different times after AVF creation. Animal weight gain was equivalent in sham and fistulated mice, indicating that AVF did not induced perturbations leading to edema.

At the time of death, mice were anesthetized as indicated earlier, and both carotid arteries were exposed, the left CCA serving as a non–operated-on internal control. The arteries were photographed *in situ*, alongside a 460 μm-wide scale placed parallel to the vessel, with a camera (Logitech, Fremont, CA) attached to the surgical microscope (Nikon, Amstelveen, NL). Precise arterial diameters were measured with the help of image-analysis software (Histolab, Suffolk, UK).

Blood-flow velocity was measured by using a 20-MHz pulsed Doppler system (Milar, Houston, TX). The pen-probe position was adjusted to obtain a 30-degree angle with the vessel axis. Blood flow was measured 5 mm upstream of the AVF in the RCCA and at the equivalent location in the left common carotid artery. Velocities (V, cm/s) were obtained from the measured Doppler frequency shifts, and volume flow (Q) was calculated by multiplying the mean velocity by the cross-sectional area of the vessel lumen, by using the formula Q (cm^3/s) $= \pi r^2$ V, where r is the radius in cm. Wall shear stress was calculated by using the Poiseuille formula, $\tau = 4\,\mu\,Q/\pi\,r^3$. In this formula, μ is the viscosity of blood (taken to be 0.035 poise).

Histologic analysis

After hemodynamic measurements, animals were killed with a bolus injection of sodium pentobarbital (0.5 mg/kg IV). Blood was washed out of the vasculature by perfusion at 100 mm Hg with normal saline solution through a cannula inserted in the abdominal artery. Arterial segments were embedded vertically in Tissue-tek (Sakura, Tokyo, Japan), and serial 10-μm sections were cut. Phospho-p65 NF-κB (S529) was detected by using a polyclonal antibody (Rockland, Gilbertsville, PA), offset by DAPI mounting medium. ROS were detected by using dihydroethidine (tissue sections) and L-012 (tissue lysates), as described previously (27). MMP-9 was detected by using a primary rabbit polyclonal antibody (Santa Cruz). For *in situ* zymography, vessel sections were incubated at 37°C for 24 h in DQ gelatin (28). All sections are shown with the adventitia facing down and the luminal aspect facing up. Semiquantitative analysis of gelatinase fluorescence was done independently by two individuals with Histolab software.

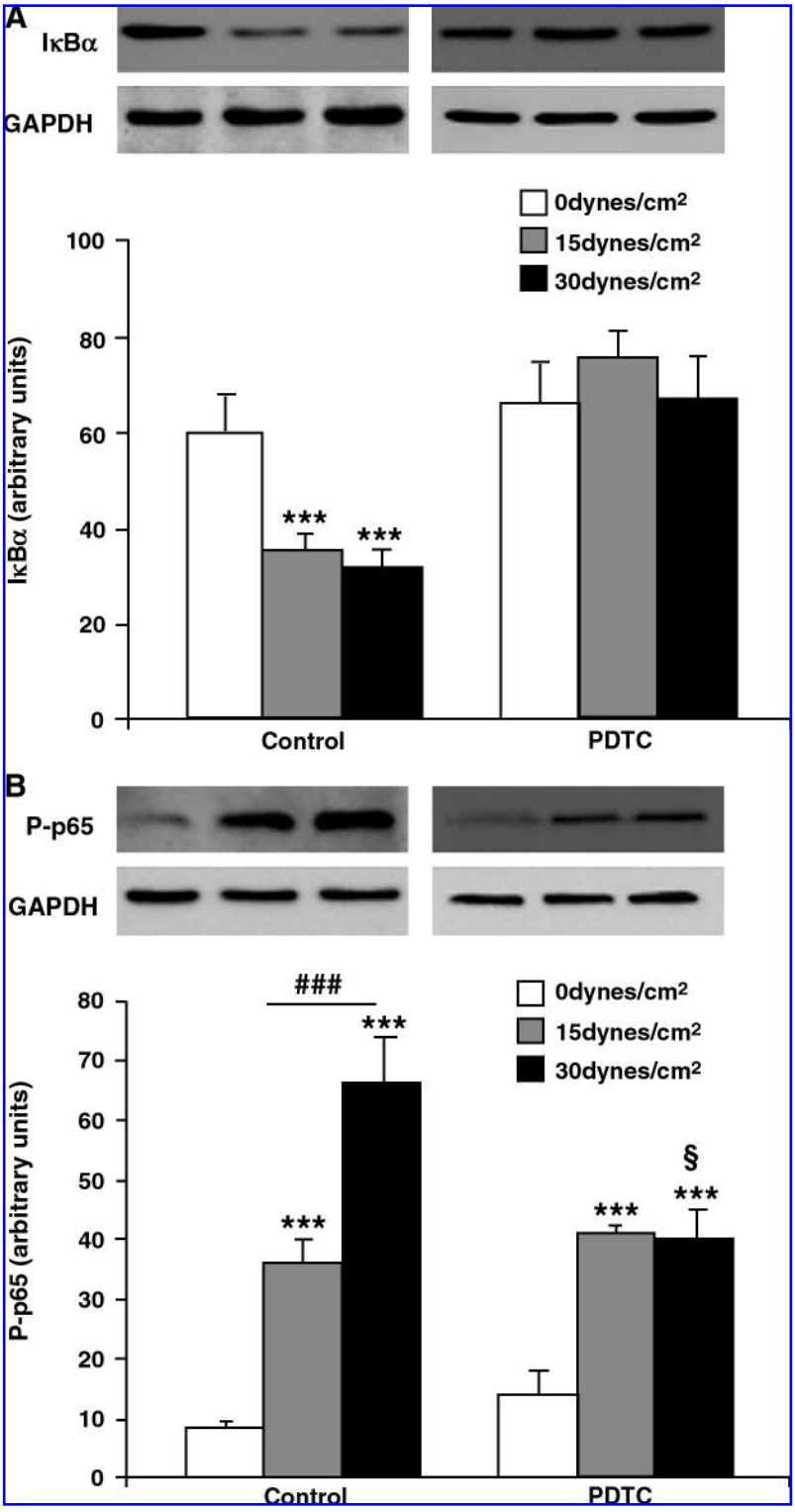

FIG. 1. Shear stress induces the NF-κB pathway in endothelial cells. (**A**) The NF-κB inhibitor IκBα was degraded in ECs exposed to 15 or 30 dynes/cm^2 for 24 h. This effect was blocked by 10^{-6} *M* PDTC treatment. (**B**) Phosphorylation of the p65 subunit of NF-κB was enhanced in endothelial cells at 15 dynes/cm^2 and even more in cells at 30 dynes/cm^2. PDTC inhibited the supplemental phosphorylation of p65 due to very high shear stress only. Results are expressed as mean ± SEM of $n = 6$. ***$p < 0.001$ *vs.* 0 dynes/cm^2; ###$p < 0.001$ *vs.* 15 dynes/cm^2; §$p < 0.05$ *vs.* 30 dynes/cm^2, no PDTC.

Luminescence assay

Vessel ROS levels were quantified by using L-012, as described recently (6). Carotid arteries were lysed in 50 m*M* Tris buffer (pH 7.5) containing protease inhibitors (Boehringer) and lysates centrifuged at 10,000 *g* for 15 min at 4°C. Supernatants were then incubated with 100 μ*M* L-012 (Wako, Osaka, Japan) and luminescence counted (Perkin Elmer Topcount NXT, Waltham, MA) for 5 s after a 10-min interval, allowing the plates to become adapted to the dark.

Statistical analysis

Results are expressed as mean ± SEM. Data were analyzed by one-way (for comparison of control *vs.* AVF) or two-way ANOVA (for analysis-of-treatment effects). When ANOVA

analyses yielded significant results, comparisons were done by using Bonferroni's test. Differences were considered statistically significant at a value of $p < 0.05$.

Results

Prolonged shear stress induces NF-κB and MMPs in HUVECs

HUVECs were exposed to no-flow conditions or to normal (15 dynes/cm^2) or high (30 dynes/cm^2) shear stress for 24 h to assess effects on NF-κB activation and MMP production. IκBα degradation, an index of NF-κB pathway activation, was observed to be equivalent in cells exposed to high and low shear stress; protein levels of IκBα were reduced to 58 and 53% of static controls, respectively ($p < 0.001$). This effect was completely abolished by $10^{-6}\,M$ PDTC treatment (Fig. 1A). Both normal and high shear stress were also associated with increased phosphorylation of the p65 subunit of NF-κB compared with static controls ($p < 0.001$). However, the degree of phosphorylation of p65 was greater in cells exposed to high shear stress than in cells submitted to normal shear stress ($p < 0.001$), and only this incremental p65 phosphorylation appeared to be sensitive to PDTC (Fig. 1B). This supplemental phosphorylation of NF-κB coincided with increased ROS production in HUVECs exposed to high shear stress (Fig. 2). PDTC treatment prevented ROS production in all HUVECs irrespective of flow conditions, and at all concentrations tested, from $10^{-7}\,M$ to $10^{-4}\,M$ (Fig. 2). Hence, PDTC prevented IκBα degradation and p65 translocation in HUVECs maintained at 15 and 30 dynes/cm^2, but abolished p65 phosphorylation only in cells exposed to the high shear stress. Nevertheless, differences in the extent of p65 phosphorylation appeared to have no bearing on MMP-2 and MMP-9 induction, because gelatin zymography revealed equivalent activity of these enzymes in cells exposed to 15 and 30 dynes/cm^2 (Fig. 3). Rather, MMP induction appeared to follow nuclear translocation of phosphorylated p65, which presumably depended on IκBα degradation being prevented by PDTC in cells exposed to either 15 and or 30 dynes/cm^2 (Fig. 4A and B). Likewise, PDTC abolished MMP activity equally in both shear conditions, returning metalloproteinase activity to levels found in static cells (Fig. 3). These results were confirmed by *in situ* zymography in whole cells (Fig. 4).

Vascular remodeling in vessels from control and PDTC-treated mice

The role of NF-κB in vascular MMP production and remodeling was evaluated in a mouse model of AVF. As reported earlier (6), creation of a shunt between the RCCA and jugular vein produced an abrupt increase in arterial blood flow in all animals, reaching more than sixfold from the onset, and flow in the carotid artery remained consistently high during the following 3 weeks. Neither the blood pressure nor the heart rate was altered by the AVF (data not shown), and no changes in blood flow or vessel diameter (Fig. 5) were observed in the contralateral artery. Shear stress, calculated at 39 ± 2 dynes/cm^2 before AVF, was maximal the first day (278 ± 7 dynes/cm^2) after surgery and diminished thereafter, returning toward baseline levels as the weeks progressed (Fig. 5B). In parallel, RCCA diameter gradually increased, driven by high wall shear stress, reaching a maximum at 3 weeks (Fig. 5A). Despite the marked increases in vessel diameter, no changes in artery thickness were observed in any vessels (data not shown).

Positive staining for phospho-p65 NF-κB was detected throughout the vessel walls of RCCAs both 7 and 21 days after creation of the fistula (Fig. 6A). Mice were treated with PDTC, which effectively blocked p65 phosphorylation (Fig. 6A), to

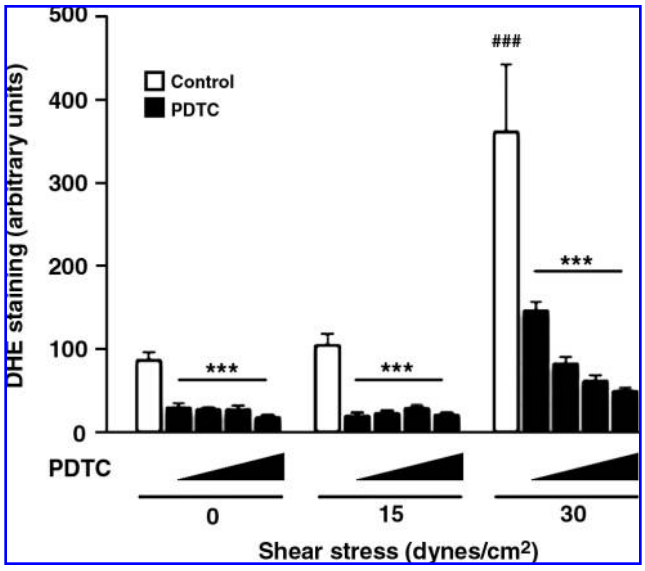

FIG. 2. PDTC prevents shear stress–induced ROS production. HUVECs were treated with incremental concentrations of PDTC (10^{-7}, 10^{-6}, 10^{-5}, $10^{-4}\,M$) and exposed to a shear stress of 0, 15, or 30 dynes/cm^2 for 24 h. ROS production was significantly enhanced in cells exposed to the high-flow condition, but in all cases, PDTC abolished ROS release. ***$p < 0.001$ *vs.* untreated at the same shear stress; ###$p < 0.001$ *vs.* 0 dynes/cm^2.

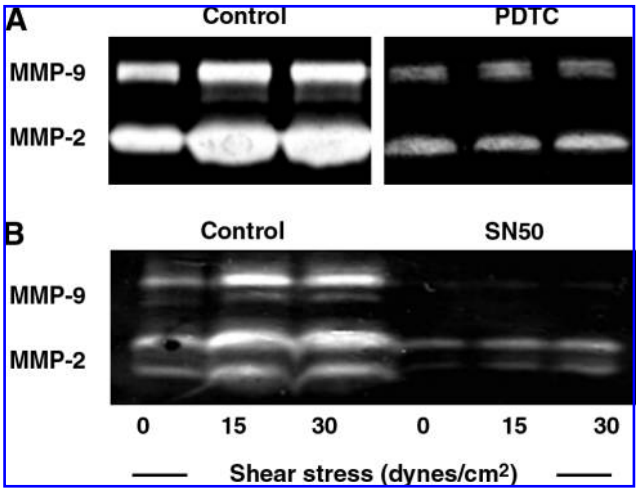

FIG. 3. MMP activity is enhanced in endothelial cells stimulated by 15 or 30 dynes/cm^2 for 24 h. Gelatin zymography of cell lysates revealed that MMP-2 and MMP-9 are induced equally by both levels of shear stress. (**A**) PDTC and (**B**) SN50 completely abolished MMP activity in all conditions. Representative of four separate experiments.

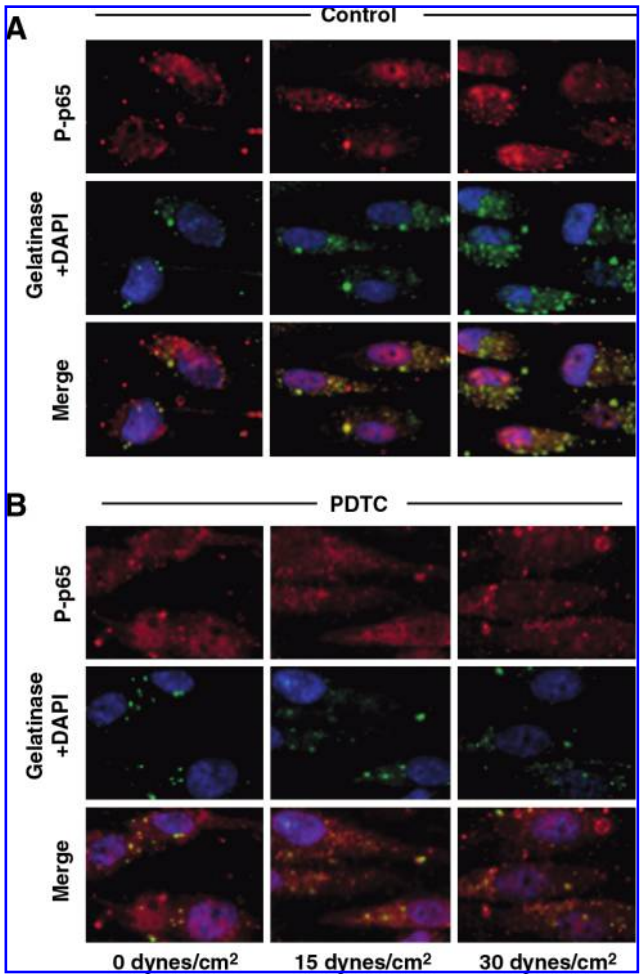

FIG. 4. (A) Immunocytochemistry and in situ zymography reveal increased nuclear localization of the phosphorylated p65 subunit of NF-κB (P-p65), shown by bright pink coloration in DAPI-stained nuclei (blue), as well as enhanced MMP activity (green DQ gelatinase fluorescence), in ECs subjected to a shear stress of 15 or 30 dynes/cm^2, compared with unstimulated cells. (B) In cells treated with PDTC, the P-p65 staining remains diffuse, and MMP activity is comparable in all cells regardless of the shear stress applied. Representative of five separate experiments. (For interpretation of the references to color in this figure legend, the reader is referred to the web version of this article at www.liebertonline.com/ars).

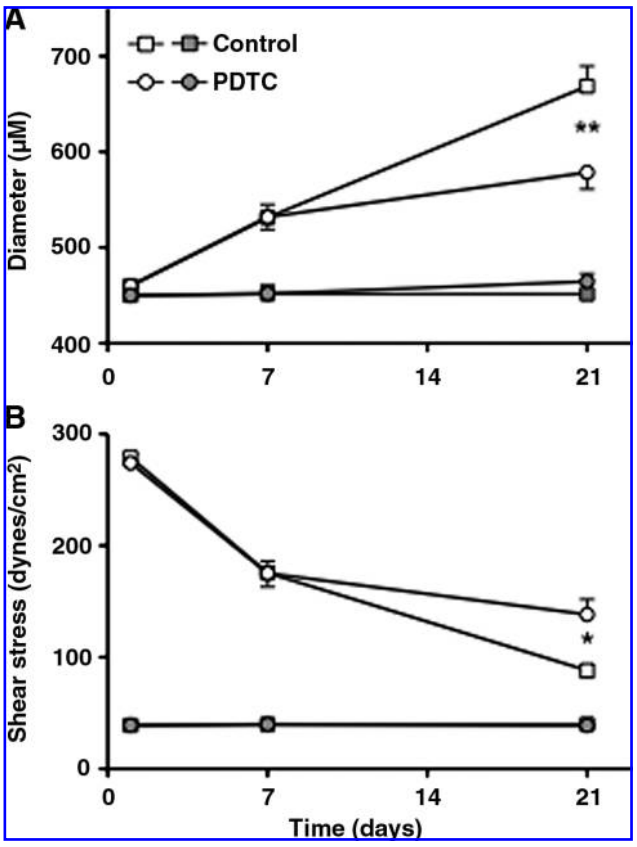

FIG. 5. The remodeling response in mouse carotid arteries before (day 0) and 7 and 21 days after AVF creation. (**A**) The carotid diameter of control animals increased gradually over a 3-week period after opening of the arteriovenous fistula. In PDTC-treated mice, remodeling was stunted after the first week, resulting in a comparatively reduced diameter at 21 days. (**B**) Shear stress in the carotid artery peaked immediately (day 1) after AVF creation and then decreased with time in control mice. However, shear stress remained elevated in mice with PDTC. Contralateral vessel diameter and shear stress did not vary at 1 and 3 weeks and did not differ between animal treatments (*gray*). Results are expressed as mean ± SEM of $n = 5$; $^*p < 0.05$, and $^{**}p < 0.01$ PDTC *vs.* control.

verify the contribution of NF-κB to flow-induced vascular remodeling. At the 1-week time point after AVF, flow-induced arterial enlargement was comparable to that in untreated animals. Accordingly, shear stress diminished similarly in both groups. However, vessel remodeling subsequently slowed in the PDTC-treated mice, such that the increase in RCCA diameter between 1 and 3 weeks was lower in these animals (8%) than in untreated controls (26%), resulting in significantly different vessel diameters ($p < 0.01$) and shear-stress values ($p < 0.05$) between these groups at the 3-week time point (Fig. 5). These results suggest that NF-κB plays a role in the delayed vascular remodeling rather than in the early phases of the process.

ROS and MMP induction in the AVF

We previously demonstrated that ROS contribute to MMP activation and vascular remodeling in the AVF model (6). In the current study, we confirmed that ROS are produced in 1- and 3-week flow-loaded vessels, demonstrated by enhanced oxy-ethidium fluorescence throughout the vascular wall of carotid artery sections incubated with dihydroethidine. These results were substantiated by L-012 luminescence, wherein ROS production in flow-loaded arteries was compared with that in contralateral vessels. In untreated mice, low levels of ROS were detected in unoperated RCCAs (day 0), but superoxide levels were significantly enhanced ($p < 0.01$) 1-week after AVF and remained elevated at the 3-week time point ($p < 0.05$; Fig. 6B and C). In flow-loaded arteries of PDTC-treated mice, ROS production in the RCCA 1 week after AVF was lower than that in untreated controls ($p < 0.05$), but it remained significant nonetheless ($p < 0.01$).

Moreover, differences in ROS production between the treatment groups did not persist at 3 weeks (Fig. 6).

In situ gelatinase activity was enhanced in flow-loaded RCCAs of untreated mice both 1 and 3 weeks after AVF (Fig. 7). However, in PDTC-treated animals, gelatinase activity was enhanced only at 1 week, returning to baseline thereafter (Fig. 7B and C), despite the fact that ROS activity remained high at this time point (Fig. 6). Reduced gelatinolytic activity did, however, coincide with lower MMP-9 expression in the vessels from PDTC-treated mice at 3 weeks, compared with untreated controls and with observations at 1 week (Fig. 7A). Hence, PDTC treatment appears to impede long-term upregulation of MMP-9, which could contribute to reduced arterial remodeling in the 7- to 21-day interval.

Discussion

In the present study, we demonstrated that the NF-κB pathway plays a key role in MMP activation and vascular remodeling in arteries exposed to high flow. Moreover, although NF-κB clearly participates in MMP synthesis and activation in endothelial cells exposed to high shear stress for 24 h, blunting NF-κB activity in the whole vessel affects not early expansion but rather long-term remodeling. Our study thus reveals that flow-induced remodeling encompasses two stages, consisting of an acute phase independent of NF-κB activity lasting $\sim$1 week, and a later, more long-term phase that requires NF-κB to proceed fully.

NF-κB activation in endothelial cells is usually associated with conditions of low or oscillatory flow (35), and NF-κB was previously reported to induce MMPs in endothelial cells exposed to low shear stress (42). At normal flow rates, NO release is expected to curtail NF-κB activation (19). For example, increased DNA-binding capacity of NF-κB in endothelial cells exposed to low shear stress was counteracted by overexpression of eNOS (34), and physiologic shear stress applied over an 18- to 24-h period abolished NF-κB activation in ECs grown in co-culture with smooth muscle cells (9) or stimulated with TNF-α (37). However, physiologic shear stress was reported transiently to induce IKK (3) and IκBα (46) in ECs, and in the current study, we found evidence of NF-κB activation in ECs exposed for 24 h to normal and high flow. Furthermore, treatment with the inhibitor peptide SN50 confirmed that NF-κB was involved in the ensuing MMP induction. The extent of p65 phosphorylation was greater in the high-flow cells, but this did not appear to influence MMP activity. Interestingly, ROS production was accentuated only in cells exposed to high shear stress, indicating that MMP activation by low flow occurred independently of supplemental ROS generation; however, the latent ROS levels may have been sufficient for ROS activation in low-flow conditions. PDTC prevented ROS generation as well as NF-κB and MMP activation at both low and high shear stresses. It is therefore possible that in the absence of proinflammatory stimuli, endothelial cells respond to a change in the flow rate through induction of the NF-κB pathway and subsequent MMP activation, regardless of the level of shear stress applied.

The remodeling process occurring in vessels exposed to prolonged elevations in blood flow comprises of two mechanical components, shear stress and tensile strain. Shear stress acting on endothelial cells is essential to the dilatory response, because de-endothelialized segments of flow-loaded rat and rabbit common carotid arteries fail to remodel (43, 45). The release of NO in this context contributes both to the immediate increase in vessel diameter (reaching 10%) (45) and to the prolonged vessel expansion that allows eventual normalization of shear stress (6, 45). Reactive oxygen species also play a part in the remodeling process. Hydrogen peroxide originating from mitochondrial respiration was found to be necessary for flow-induced dilatation in human coronary arteries (31, 33). More recently, data obtained in $p47^{phox-/-}$ mice provided direct evidence that ROS generated in fistulated arteries are necessary for their expansion (6), at least in the first week. Increased peroxynitrite, the combination of NO with O_2^-, is likely to be the major activator of MMPs in this setting (6, 38). Moreover, shear stress–induced peroxynitrite could very well explain the high NF-κB activity in fistulated vessels, because interaction of ROS with NO (41), as well as peroxynitrite generators 4-hydroxyhexenal (47) and SIN-1 (10), were all shown to activate endothelial NF-κB. Interestingly, although we found that PDTC prevented ROS generation in ECs *in vitro*, and this may have accounted for reduced NF-κB and MMP activity in response to shear stress, PDTC did not reduce ROS production in flow-loaded arteries *in vivo*, and it did not affect arterial expansion in the first week after creation of the fistula, the time frame when AVF enlargement was the most hindered by the lack of ROS in $p47^{phox-/-}$ mice (6). Hence, the effect of PDTC on the remodeling response is unlikely to have stemmed from ROS inhibition.

In fistulated vessels, shear stress is not the only mechanical force that participates in the remodeling process. Rapid degradation of the internal elastic lamina (17, 45) results in arterial distention that stretches the underlying smooth muscle cells, producing tensile strain. Increased MMP activity has been documented in smooth muscle cells (2, 18, 36, 40, 48) and whole vessels (8, 23, 28) exposed to steady or cyclic stretch, and MMP-9 was found to be essential for expansive arterial remodeling because of increased pressure both *in vivo* (15, 23) and *ex vivo* (8, 28). Interestingly, MMP-2 upregulation in smooth muscle cells exposed to cyclic stretch also depends on the presence of $p47^{phox}$ (18), indicating that NADPH oxidase–derived ROS may bridge the gap between mechanical strain and MMP production in many types of vascular cells. Furthermore, the activation of the NF-κB cascade was previously documented in stretched endothelial cells (13, 26), smooth muscle cells (7, 39), and whole vessels (11, 29), and NF-κB induction proved to be important for MMP synthesis in this context (30). Hence, circumferential wall stretch may very well contribute significantly to flow-induced arterial remodeling in our model of AVF. This would explain why NF-κB and MMPs are induced throughout the vessel wall in fistulated arteries rather than in endothelial cells alone.

The AVF is a good model in which to investigate flow-induced remodeling, which has emerged as an important contributor to arteriogenesis. Many processes associated with collateral artery growth and recovery in models of hindlimb ischemia mimic what occurs in the AVF, including increased shear stress (14), eNOS expression (5, 14), and MMP activation (4). Collateral growth in ischemic hindlimbs was found to depend on stretch-dependent activation of the AP-1 pathway (12) that can upregulate MMP-2 (9), and on proinflammatory signaling (21, 22) spearheaded by the NF-κB pathway of monocytic cell origin (32). Here we show NF-κB can originate from the flow-loaded vessel itself and stimulate MMP-9

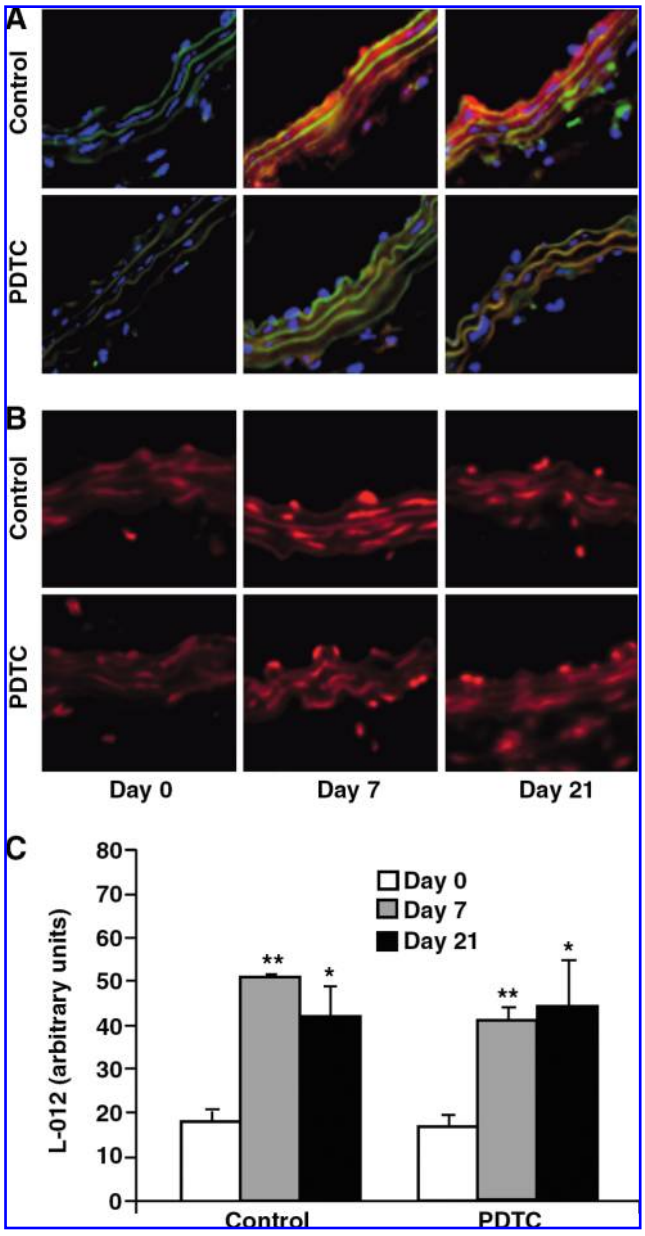

FIG. 6. Flow-loaded vessels display enhanced NF-κB activity and ROS generation. (**A**) Immunohistochemistry for phospho-p65 (red fluorescence) demonstrates that the NF-κB pathway was induced in carotid arteries of control animals 1 week after creation of the fistula and remained activated at 3 weeks. Phospho-p65 staining was greatly reduced in PDTC-treated mice. Elastic laminas are shown as green autofluorescence, and nuclei are stained blue with DAPI. (**B**) Superoxide formation evaluated by dihydroethidine staining in RCCAs obtained before (day 0) and 7 and 21 days after AVF reveals increased ROS production in the endothelium and throughout the vessel wall of control and PDTC-treated animals, at 1 and 3 weeks, with no apparent differences between treatment groups. (**C**) This is substantiated by an L-012 luminescence assay of whole-vessel lysates, showing equivalent levels of ROS in all fistulated vessels. Original magnification, x20. Results are expressed as mean ± SEM of $n = 3$–5; $^{*}p < 0.05$ and $^{**}p < 0.01$ *vs.* day 0. (For interpretation of the references to color in this figure legend, the reader is referred to the web version of this article at www.liebertonline.com/ars).

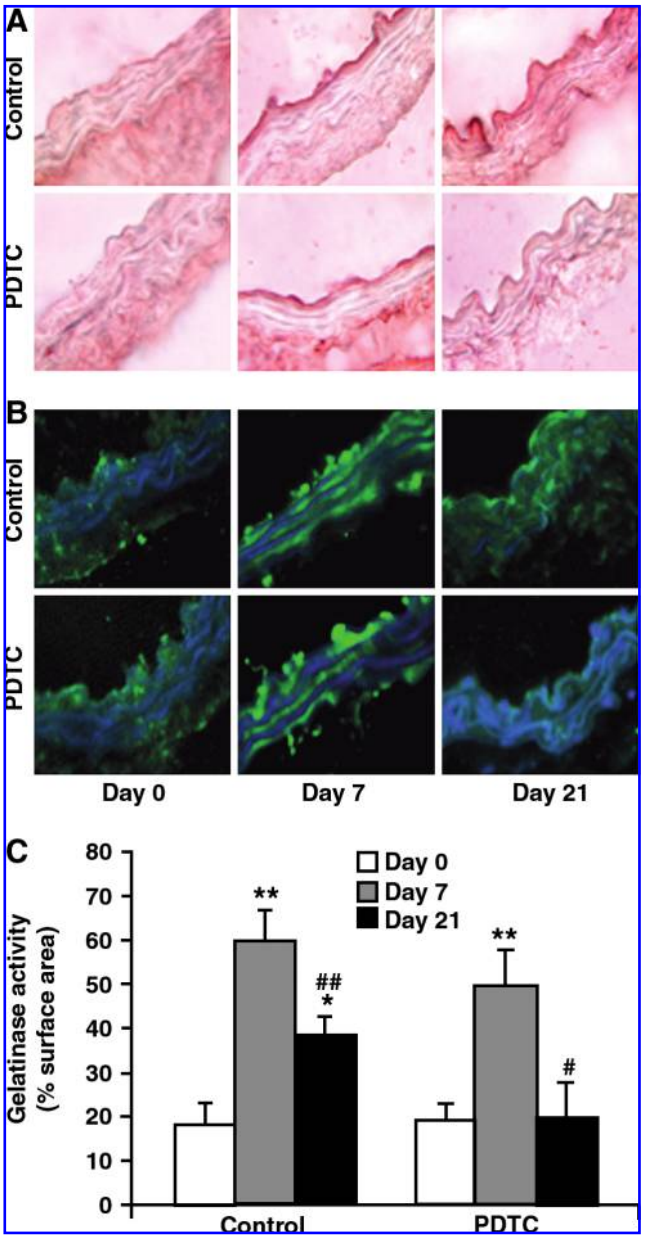

FIG. 7. High flow is associated with upregulation of MMP-9. (**A**) One and 3 weeks after AVF creation, MMP-9 staining is enhanced in the innermost artery layers of control mice, compared with day 0. In vessels of PDTC-treated mice, however, no MMP-9 is detectable at day 21. (**B**) *In situ* gelatinase assay reveals high MMP activity (green fluorescence) in the endothelium and medial portions of flow-loaded arteries. Fluorescence was equally enhanced in RCCAs of control and PDTC-treated mice 7 days after AVF, but at 21 days, only the control animals still manifested enhanced MMP activity. Autofluorescent elastic laminas appear as blue bands. (**C**) Semiquantitative analysis of gelatinase fluorescence in the vessel wall. Original magnification, ×20. Results are expressed as mean ± SEM of $n = 5$; $^{*}p < 0.05$ and $^{**}p < 0.01$ *vs.* day 0; $\#p < 0.05$ and $\#\#p < 0.01$ *vs.* day 7. (For interpretation of the references to color in this figure legend, the reader is referred to the web version of this article at www.liebertonline.com/ars).

therein. Our data may therefore help identify the steps involved in arteriogenesis in ischemic tissues.

In summary, NF-κB appears to play an extensive role in blood flow–induced vascular remodeling in the mouse carotid fistula model. It is probable that activation of this pathway in the vascular wall contributes to the synthesis of MMPs and other key mediators, allowing long-term structural adaptation to altered blood flow.

Acknowledgments

The first two authors contributed equally to the work presented herein.

This work emanates from the European Vascular Genomics Network (http://www.evgn.org), a Network of Excellence supported by the European Community's sixth Framework Programme for Research Priority 1 "Life Sciences, Genomics and Biotechnology for Health" (Contract LSHM-CT-2003-503254).

Abbreviations

AVF, arteriovenous fistula; EC, endothelial cell; eNOS, endothelial nitric oxide synthase; HUVEC, human umbilical vein endothelial cell; IκBα, inhibitor κBα; MMP, metalloproteinase; MT1-MMP, membrane-type metalloproteinase 1; NF-κB, nuclear factor κB; NO, nitric oxide; PDTC, pyrrolidine dithiocarbamate; RCCA, right common carotid artery; ROS, reactive oxygen species; TNF-α, tumor necrosis factor α.

Disclosure Statement

No competing financial interests exist.

References

1. Abbruzzese TA, Guzman RJ, Martin RL, Yee C, Zarins CK, and Dalman RL. Matrix metalloproteinase inhibition limits arterial enlargements in a rodent arteriovenous fistula model. *Surgery* 124: 328–334, 1998.
2. Asanuma K, Magid R, Johnson C, Nerem RM, and Galis ZS. Uniaxial strain upregulates matrix-degrading enzymes produced by human vascular smooth muscle cells. *Am J Physiol Heart Circ Physiol* 284: H1778–H1784, 2003.
3. Bhullar IS, Li YS, Miao H, Zandi E, Kim M, Shyy JY, and Chien S. Fluid shear stress activation of Ikappab kinase is integrin-dependent. *J Biol Chem* 273: 30544–30549, 1998.
4. Cai H and Harrison DG. Endothelial dysfunction in cardiovascular diseases: the role of oxidant stress. *Circ Res* 87: 840–844, 2000.
5. Cai WJ, Kocsis E, Luo X, Schaper W, and Schaper J. Expression of endothelial nitric oxide synthase in the vascular wall during arteriogenesis. *Mol Cell Biochem* 264: 193–200, 2004.
6. Castier Y, Brandes RP, Leseche G, Tedgui A, and Lehoux S. p47phox-Dependent NADPH oxidase regulates flow-induced vascular remodeling. *Circ Res* 97: 533–540, 2005.
7. Chaqour B, Howard PS, Richards CF, and Macarak EJ. Mechanical stretch induces platelet-activating factor receptor gene expression through the NF-kappaB transcription factor. *J Mol Cell Cardiol* 31: 1345–1355, 1999.
8. Chesler NC, Ku DN, and Galis ZS. Transmural pressure induces matrix-degrading activity in porcine arteries ex vivo. *Am J Physiol* 277: H2002–H2009, 1999.
9. Chiu JJ, Chen LJ, Chang SF, Lee PL, Lee CI, Tsai MC, Lee DY, Hsieh HP, Usami S, and Chien S. Shear stress inhibits smooth muscle cell-induced inflammatory gene expression in endothelial cells: role of NF-kappaB. *Arterioscler Thromb Vasc Biol* 25: 963–969, 2005.
10. Cooke CL and Davidge ST. Peroxynitrite increases iNOS through NF-kappaB and decreases prostacyclin synthase in endothelial cells. *Am J Physiol Cell Physiol* 282: C395–C402, 2002.
11. Csiszar A, Smith KE, Koller A, Kaley G, Edwards JG, and Ungvari Z. Regulation of bone morphogenetic protein-2 expression in endothelial cells: role of nuclear factor-kappaB activation by tumor necrosis factor-alpha, H_2O_2, and high intravascular pressure. *Circulation* 111: 2364–2372, 2005.
12. Demicheva E, Hecker M, and Korff T. Stretch-induced activation of the transcription factor activator protein-1 controls monocyte chemoattractant protein-1 expression during arteriogenesis. *Circ Res* 103: 477–484, 2008.
13. Du W, Mills I, and Sumpio BE. Cyclic strain causes heterogeneous induction of transcription factors, ap-1, cre binding protein and NF-κB, in endothelial cells: species and vascular bed diversity. *J Biomech* 28: 1485–1491, 1995.
14. Eitenmuller I, Volger O, Kluge A, Troidl K, Barancik M, Cai WJ, Heil M, Pipp F, Fischer S, Horrevoets AJ, Schmitz-Rixen T, and Schaper W. The range of adaptation by collateral vessels after femoral artery occlusion. *Circ Res* 99: 656–662, 2006.
15. Flamant M, Placier S, Dubroca C, Esposito B, Lopes I, Chatziantoniou C, Tedgui A, Dussaule JC, and Lehoux S. Role of matrix metalloproteinases in early hypertensive vascular remodeling. *Hypertension* 50: 212–218, 2007.
16. Gambillara V, Montorzi G, Haziza-Pigeon C, Stergiopulos N, and Silacci P. Arterial wall response to ex vivo exposure to oscillatory shear stress. *J Vasc Res* 42: 535–544, 2005.
17. Greenhill NS and Stehbens WE. Scanning electron microscopic investigation of the afferent arteries of experimental femoral arteriovenous fistulae in rabbits. *Pathology* 19: 22–27, 1987.
18. Grote K, Flach I, Luchtefeld M, Akin E, Holland SM, Drexler H, and Schieffer B. Mechanical stretch enhances mRNA expression and proenzyme release of matrix metalloproteinase-2 (MMP-2) via NAD(P)H oxidase-derived reactive oxygen species. *Circ Res* 92: e80–e86, 2003.
19. Grumbach IM, Chen W, Mertens SA, and Harrison DG. A negative feedback mechanism involving nitric oxide and nuclear factor kappa-B modulates endothelial nitric oxide synthase transcription. *J Mol Cell Cardiol* 39: 595–603, 2005.
20. Guzman RJ, Abe K, and Zarins CK. Flow-induced arterial enlargement is inhibited by suppression of nitric oxide synthase activity in vivo. *Surgery* 122: 273–279, 1997.
21. Heil M and Schaper W. Influence of mechanical, cellular, and molecular factors on collateral artery growth (arteriogenesis). *Circ Res* 95: 449–458, 2004.
22. Hoefer IE, van Royen N, Rectenwald JE, Deindl E, Hua J, Jost M, Grundmann S, Voskuil M, Ozaki CK, Piek JJ, and Buschmann IR. Arteriogenesis proceeds via ICAM-1/mac-1-mediated mechanisms. *Circ Res* 94: 1179–1185, 2004.
23. Jackson ZS, Gotlieb AI, and Langille BL. Wall tissue remodeling regulates longitudinal tension in arteries. *Circ Res* 90: 918–925, 2002.
24. Karwowski JK, Markezich A, Whitson J, Abbruzzese TA, Zarins CK, and Dalman RL. Dose-dependent limitation of arterial enlargement by the matrix metalloproteinase inhibitor rs-113,456. *J Surg Res* 87: 122–129, 1999.
25. Kim JI, Cordova AC, Hirayama Y, Madri JA, and Sumpio BE. Differential effects of shear stress and cyclic strain on sp1

phosphorylation by protein kinase Czeta modulates membrane type 1-matrix metalloproteinase in endothelial cells. *Endothelium* 15: 33–42, 2008.
26. Kobayashi S, Nagino M, Komatsu S, Naruse K, Nimura Y, Nakanishi M, and Sokabe M. Stretch-induced IL-6 secretion from endothelial cells requires NF-kappaB activation. *Biochem Biophys Res Commun* 308: 306–312, 2003.
27. Lehoux S, Esposito B, Merval R, Loufrani L, and Tedgui A. Pulsatile stretch-induced extracellular signal-regulated kinase 1/2 activation in organ culture of rabbit aorta involves reactive oxygen species. *Arterioscler Thromb Vasc Biol* 20: 2366–2372, 2000.
28. Lehoux S, Lemarie CA, Esposito B, Lijnen HR, and Tedgui A. Pressure-induced matrix metalloproteinase-9 contributes to early hypertensive remodeling. *Circulation* 109: 1041–1047, 2004.
29. Lemarie CA, Esposito B, Tedgui A, and Lehoux S. Pressure-induced vascular activation of nuclear factor-kappaB: role in cell survival. *Circ Res* 93: 207–212, 2003.
30. Lemarie CA, Tharaux PL, Esposito B, Tedgui A, and Lehoux S. Transforming growth factor-alpha mediates nuclear factor kappaB activation in strained arteries. *Circ Res* 99: 434–441, 2006.
31. Liu Y, Zhao H, Li H, Kalyanaraman B, Nicolosi AC, and Gutterman DD. Mitochondrial sources of H_2O_2 generation play a key role in flow-mediated dilation in human coronary resistance arteries. *Circ Res* 93: 573–580, 2003.
32. Luo D, Luo Y, He Y, Zhang H, Zhang R, Li X, Dobrucki WL, Sinusas AJ, Sessa WC, and Min W. Differential functions of tumor necrosis factor receptor 1 and 2 signaling in ischemia-mediated arteriogenesis and angiogenesis. *Am J Pathol* 169: 1886–1898, 2006.
33. Miura H, Bosnjak JJ, Ning G, Saito T, Miura M, and Gutterman DD. Role for hydrogen peroxide in flow-induced dilation of human coronary arterioles. *Circ Res* 92: e31–e40, 2003.
34. Mohan S, Hamuro M, Sorescu GP, Koyoma K, Sprague EA, Jo H, Valente AJ, Prihoda TJ, and Natarajan M. IkappaBalpha-dependent regulation of low-shear flow-induced NF-kappa B activity: role of nitric oxide. *Am J Physiol Cell Physiol* 284: C1039–C1047, 2003.
35. Nagel T, Resnick N, Dewey CF Jr, and Gimbrone MA Jr. Vascular endothelial cells respond to spatial gradients in fluid shear stress by enhanced activation of transcription factors. *Arterioscler Thromb Vasc Biol* 19: 1825–1834, 1999.
36. O'Callaghan CJ and Williams B. Mechanical strain-induced extracellular matrix production by human vascular smooth muscle cells: role of TGF-beta(1). *Hypertension* 36: 319–324, 2000.
37. Partridge J, Carlsen H, Enesa K, Chaudhury H, Zakkar M, Luong L, Kinderlerer A, Johns M, Blomhoff R, Mason JC, Haskard DO, and Evans PC. Laminar shear stress acts as a switch to regulate divergent functions of NF-kappaB in endothelial cells. *FASEB J* 21: 3553–3561, 2007.
38. Rajagopalan S, Meng XP, Ramasamy S, Harrison DG, and Galis ZS. Reactive oxygen species produced by macrophage-derived foam cells regulate the activity of vascular matrix metalloproteinases in vitro: implications for atherosclerotic plaque stability. *J Clin Invest* 98: 2572–2579, 1996.
39. Schulze PC, De Keulenaer GW, Kassik KA, Takahashi T, Chen Z, Simon DI, and Lee RT. Biomechanically induced gene iex-1 inhibits vascular smooth muscle cell proliferation and neointima formation. *Circ Res* 93: 1210–1217, 2003.
40. Seliktar D, Nerem RM, and Galis ZS. The role of matrix metalloproteinase-2 in the remodeling of cell-seeded vascular constructs subjected to cyclic strain. *Ann Biomed Eng* 29: 923–934, 2001.
41. Sohn HY, Krotz F, Zahler S, Gloe T, Keller M, Theisen K, Schiele TM, Klauss V, and Pohl U. Crucial role of local peroxynitrite formation in neutrophil-induced endothelial cell activation. *Cardiovasc Res* 57: 804–815, 2003.
42. Sun HW, Li CJ, Chen HQ, Lin HL, Lv HX, Zhang Y, and Zhang M. Involvement of integrins, MAPK, and NF-kappaB in regulation of the shear stress-induced MMP-9 expression in endothelial cells. *Biochem Biophys Res Commun* 353: 152–158, 2007.
43. Tohda K, Masuda H, Kawamura K, and Shozawa T. Difference in dilatation between endothelium-preserved and -desquamated segments in the flow-loaded rat common carotid artery. *Arterioscler Thromb* 12: 519–528, 1992.
44. Tronc F, Mallat Z, Lehoux S, Wassef M, Esposito B and Tedgui A. Role of matrix metalloproteinases in blood flow-induced arterial enlargement. *Arterioscler Thromb Vasc Biol* 20: e120–e126, 2000.
45. Tronc F, Wassef M, Esposito B, Henrion D, Glagov S, and Tedgui A. Role of NO in flow-induced remodeling of the rabbit common carotid artery. *Arterioscler Thromb Vasc Biol* 16: 1256–1262, 1996.
46. Wang Y, Chang J, Li YC, Li YS, Shyy JY, and Chien S. Shear stress and VEGF activate IKK via the flk-1/cbl/akt signaling pathway. *Am J Physiol Heart Circ Physiol* 286: H685–H692, 2004.
47. Wessels MW, Catsman-Berrevoets CE, Mancini GM, Breuning MH, Hoogeboom JJ, Stroink H, Frohn-Mulder I, Coucke PJ, Paepe AD, Niermeijer MF, and Willems PJ. Three new families with arterial tortuosity syndrome. *Am J Med Genet A* 131A: 134–143, 2004.
48. Yang JH, Briggs WH, Libby P, and Lee RT. Small mechanical strains selectively suppress matrix metalloproteinase-1 expression by human vascular smooth muscle cells. *J Biol Chem* 273: 6550–6555, 1998.
49. Yun S, Dardik A, Haga M, Yamashita A, Yamaguchi S, Koh Y, Madri JA, and Sumpio BE. Transcription factor sp1 phosphorylation induced by shear stress inhibits membrane type 1-matrix metalloproteinase expression in endothelium. *J Biol Chem* 277: 34808–34814, 2002.

Address reprint requests to:
Stephanie Lehoux
Lady Davis Institute for Medical Research
McGill University
3755 Cote Ste Catherine
Montreal, QC H3T 1E2

E-mail: stephanie.lehoux@mcgill.ca

Date of first submission to ARS Central, December 3, 2008; date of final revised submission, March 23, 2009; date of acceptance, March 25, 2009.

This article has been cited by:

1. Stephen J. White, Elaine M. Hayes, Stéphanie Lehoux, Jamie Y. Jeremy, Anton J.G. Horrevoets, Andrew C. Newby. 2011. Characterization of the differential response of endothelial cells exposed to normal and elevated laminar shear stress. *Journal of Cellular Physiology* **226**:11, 2841-2848. [CrossRef]
2. SBA Cau, DA Guimaraes, E Rizzi, CS Ceron, LL Souza, CR Tirapelli, RF Gerlach, JE Tanus-Santos. 2011. Pyrrolidine dithiocarbamate downregulates vascular matrix metalloproteinases and ameliorates vascular dysfunction and remodeling in renovascular hypertension. *British Journal of Pharmacology* no-no. [CrossRef]
3. Philip Webster, Lareina Wujanto, Cyril Fisher, Marjorie Walker, Rathi Ramakrishnan, Kikkeri Naresh, J. Meirion Thomas, Vassilios Papalois, Jeremy Crane, David Taube, Neill Duncan. 2011. Malignancies Confined to Disused Arteriovenous Fistulae in Renal Transplant Patients: An Important Differential Diagnosis. *American Journal of Nephrology* **34**:1, 42-48. [CrossRef]
4. Nwe Nwe Soe, Bradford C. Berk. 2011. Cyclophilin A: A Mediator of Cardiovascular Pathology. *Journal of the Korean Society of Hypertension* **17**:4, 133. [CrossRef]
5. Catherine A. Lemarié, Pierre-Louis Tharaux, Stéphanie Lehoux. 2010. Extracellular matrix alterations in hypertensive vascular remodeling. *Journal of Molecular and Cellular Cardiology* **48**:3, 433-439. [CrossRef]
6. Yassar A. Qureshi, Dirk C. Strauss, Khin Thway, Cyril Fisher, J. Meirion Thomas. 2010. Angiosarcoma developing in a non-functioning arteriovenous fistula post-renal transplant. *Journal of Surgical Oncology* n/a-n/a. [CrossRef]